

Supplementary Information

16-vertex *Oblato-Hypho-Titanaborane* $[(\text{Cp}^*\text{Ti})_2\text{B}_{14}\text{H}_{18}]$

Sourav Kar,^{+a} Subhash Bairagi,^{+a} Jean-François Halet^{*b} and Sundargopal Ghosh^{*a}

^aDepartment of Chemistry, Indian Institute of Technology Madras, Chennai 600036, India, E-mail: sghosh@iitm.ac.in

^bCNRS–Saint-Gobain–NIMS, IRL 3629, Laboratory for Innovative Key Materials and Structures (LINK), National Institute for Materials Science (NIMS), Tsukuba 305-0044, Japan, E-mail: jean-francois.halet@univ-rennes1.fr

⁺These authors contributed equally to this work.

Table of contents

I	Experimental Details	S4
I.1	Supplementary Data	
Scheme S1	Synthesis of 16-vertex <i>oblato-hypho</i> titanaboranes 1 and 2 , and complex 3 .	S5
Figure S1	Molecular structure and atom labelling diagram of 2 .	S5
Figure S2	Molecular structure and atom labelling diagram of 3 .	S6
I.2	Spectroscopic Details	
Figure S3	ESI-MS spectrum of 1 .	S7
Figure S4	^1H NMR spectrum of 1 .	S7
Figure S5	$^1\text{H}\{^{11}\text{B}\}$ NMR spectrum of 1 .	S8
Figure S6	$^{11}\text{B}\{^1\text{H}\}$ NMR spectrum of 1 .	S8
Figure S7	^{11}B NMR spectrum of 1 .	S9
Figure S8	$^{13}\text{C}\{^1\text{H}\}$ NMR spectrum of 1 .	S9
Figure S9	^1H - ^{11}B HSQC NMR spectrum of 1 .	S10
Figure S10	IR spectrum of 1 .	S10
Figure S11	ESI-MS spectrum of 2 .	S11
Figure S12	^1H NMR spectrum of 2 .	S11
Figure S13	$^1\text{H}\{^{11}\text{B}\}$ NMR spectrum of 2 .	S12
Figure S14	$^{11}\text{B}\{^1\text{H}\}$ NMR spectrum of 2 .	S12
Figure S15	^{11}B NMR spectrum of 2 .	S13
Figure S16	$^{13}\text{C}\{^1\text{H}\}$ NMR spectrum of 2 .	S13
Figure S17	^1H - ^{11}B HSQC NMR spectrum of 2 .	S14
Figure S18	IR spectrum of 2 .	S14
Figure S19	Combined UV-vis spectra of 1 and 2 .	S15
Figure S20	^1H NMR spectrum of 3 .	S15
Figure S21	$^{13}\text{C}\{^1\text{H}\}$ NMR spectrum of 3 .	S16
I.2	X-ray Analysis Details	S16
II	Computational Details	S16
Table S1	Bond parameters of $[(\text{Cp}^*\text{Ti})_2\text{B}_{14}\text{H}_{18}]$ (1) and $[(\text{Cp}^*\text{Ti})_2\text{B}_{14}\text{H}_{17}\text{Me}]$ (2) are compared with their optimized values.	S17
Figure S22	Selected molecular orbitals of 1 .	S18
Figure S23	Selected molecular orbitals of 2 .	S18
Figure S24	B–H–B and B–Me interactions in 2 obtained from NBO analysis.	S18
Figure S25	Contour-line diagram of the Laplacian of the electron density of 2 in the B11–H–B12 and Ti1–B9–B10–Ti2 plane.	S19
Figure S26	(a) HOMO of $[\text{B}_{12}\text{H}_{10}]^{4-}$ depicting localized orbitals on two adjacent bare boron atoms; (b) and (c) NBO analysis of $[\text{B}_{12}\text{H}_{10}]^{4-}$ depicted lone pairs on two adjacent bare boron atoms.	S19

Table S2	Calculated natural charges (q_{Ti} , and q_{B}), natural valence populations (Pop) and HOMO–LUMO gaps of 1 and 2 .	S20
III	Cartesian Coordinates of all Optimized Structures	
Figure S27	Optimized geometry of 1 .	S21
Figure S28	Optimized geometry of 2 .	S22
Figure S29	Optimized geometry of $[\text{B}_{12}\text{H}_{10}]^{4-}$.	S23
Figure S30	Optimized geometry of $[\text{B}_{12}\text{H}_{10}]^{2-}$.	S23
IV	References	S24

I Experimental Details

General Procedures and Instrumentation

All the manipulations were conducted under an Ar/N₂ atmosphere by using standard Schlenk line techniques or in a glove box. Solvents were distilled prior to use under an Ar atmosphere. LiBH₄ (2.0 M in THF) and [BH₃·SMe₂] were used as received (Sigma Aldrich). [Cp*TiCl₃]¹ was synthesized according to the literature methods. Thin layer chromatography was carried out on 250-μm diameter aluminum supported silica gel TLC plates (MERCK TLC Plates) to separate the reaction mixtures. NMR spectra were recorded on 500 MHz Bruker FT-NMR spectrometer. The residual solvent protons were used as reference (Benzene-d₆, δ = 7.16 ppm; Toluene-d₈, δ = 2.08, 6.97, 7.01, and 7.09 ppm), while a sealed tube that contained [Bu₄N(B₃H₈)]² in [D₆] benzene (δ_B = -30.07 ppm) was used as an external reference for the ¹¹B{¹H} NMR analysis. ¹¹B{¹H} NMR spectra were processed with a backward linear prediction algorithm to eliminate the broad ¹¹B background signal of the NMR tube.³ The mass spectrum was recorded on Qtof Micro YA263 HRMS and 6545 Qtof LC/MS instruments. Infrared (IR) spectrum was recorded with a JASCO FT/IR-400 spectrometer. UV-vis absorption spectrum was recorded on a Thermo Scientific (Evolution 300) UV-vis spectrometer.

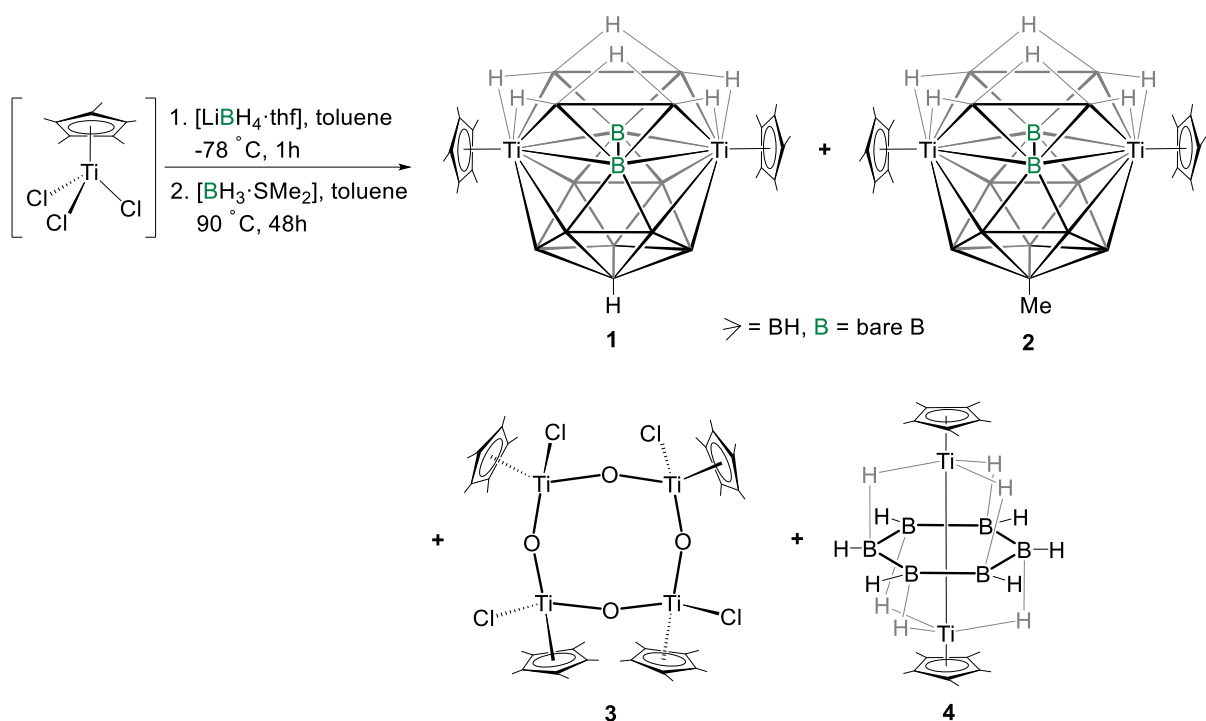
Synthesis of 1-3: In a flame-dried Schlenk tube, [(Cp*TiCl₃] (0.100 g, 0.35 mmol) was suspended in 20 mL dry toluene and it was charged with lithium borohydride solution 2.0 M in THF (0.6 mL, 1.2 mmol) dropwise at -78 °C and kept under constant stirring for 1 h. To this in situ generated intermediate, an excess amount of [BH₃·SMe₂] (1.8 mL, 1.8 mmol) was added and kept at 90 °C for 48 h under stirring condition. After addition of [BH₃·SMe₂], the mixture becomes light green. Further, during thermolysis the reaction mixture slowly converted to brown from light green and after 48 h changed to dark brown. After the completion of the reaction, the solvent was removed under vacuum. The residue was extracted with hexane/dichloromethane mixture (60:40 v/v) through a frit using 3 cm of celite. The filtrate was concentrated and the residue was subjected to chromatographic workup on 250-μm diameter aluminium-supported silica gel TLC plates (MERCK TLC Plates). Note that we have done the chromatographic workup using TLC plates inside beakers which were filled with Ar before and after filling with properly distilled eluting solvents. Elution with a hexane/dichloromethane (60:40 v/v) mixture yielded dark green **1** (0.037 g, 38%), dark green **2** (0.011 g, 11%) and pale yellow **3** (0.003 g, 4%) along with previously reported triple-decker sandwich complex [(Cp*Ti)₂(μ-η⁶:η⁶-B₆H₆)(μ-H)₆]⁴ (**4**) (0.002 g, 3%).

1: MS (ESI⁺): *m/z* calculated for [C₂₀H₄₈B₁₄Ti₂ + Na]⁺: 558.4040, found: 558.3986; ¹H NMR (500 MHz, CDCl₃, 22 °C): δ = 5.78 (br, B-Ht), 4.20 (br, B-Ht), 2.31 (br, B-Ht), 2.26 (s, 30H, 2Cp*), -0.05 (br, 2H, B-H-B), -2.59 (br, 4H, Ti-H-B) ppm; ¹¹B{¹H} NMR (160 MHz, C₆D₆, 22 °C): δ = 43.3 (br, 2B), 38.7 (br, 4B), 37.2 (br, 2B), 34.2 (br, 2B), 24.5 (br, 4B) ppm; ¹³C{¹H} NMR (125 MHz, CDCl₃, 22 °C): δ = 130.59 (C₅Me₅), 14.20 (C₅Me₅) ppm; IR (KBr, cm⁻¹): $\bar{\nu}$ = 2955, 2924, 2855, 2516 (B-H_t), 2410 (B-H_t), 2361 (B-H_t), 2070 (B-H_b), 1635, 1461, 1423, 1376, 1264, 1094, 1020, 893, 740; UV-Vis (CH₂Cl₂): λ = 268, 426 nm.

2: MS (ESI⁺): *m/z* calculated for [C₂₁H₅₀B₁₄Ti₂ + Na]⁺: 573.4169, found: 573.4158; ¹H NMR (500 MHz, CDCl₃, 22 °C): δ = 5.66 (br, B-Ht), 4.16 (br, B-Ht), 2.28 (br, B-Ht), 2.24 (s, 30H, 2Cp*), 0.51 (s, 3H, 1CH₃), -0.05 (br, 2H, B-H-B), -0.53 (br, 4H, Ti-H-B) ppm; ¹¹B{¹H} NMR (160 MHz, C₆D₆, 22 °C): δ = 52.7 (br, 1B), 41.6 (br, 1B), 38.6 (br, 4B), 36.7 (br, 2B), 35.7 (br, 2B), 35.0 (br, 4B) ppm; ¹³C{¹H} NMR (125 MHz, CDCl₃, 22 °C): δ = 130.1 (C₅Me₅), 14.1 (C₅Me₅) ppm; IR (KBr, cm⁻¹): $\bar{\nu}$ = 2956, 2927, 2849, 2520 (B-H_t), 2413 (B-H_t), 2363 (B-H_t), 2037 (B-H_b), 1724, 1641, 1460, 1377, 1262, 1089, 1018, 895, 742; UV-Vis (CH₂Cl₂): λ = 268, 430 nm.

3: ¹H NMR (500 MHz, CDCl₃, 22 °C): δ = 2.15 (s, 60H, 4Cp*) ppm; ¹³C{¹H} NMR (125 MHz, CDCl₃, 22 °C): δ = 129.0 (C₅Me₅), 12.5 (C₅Me₅) ppm.

I.1 Supplementary Data



Scheme S1. Synthesis of 16-vertex *oblato-hypho* titanaboranes **1** and **2**, and $[Cp^*TiCl(\mu-O)]_4$ (**3**).

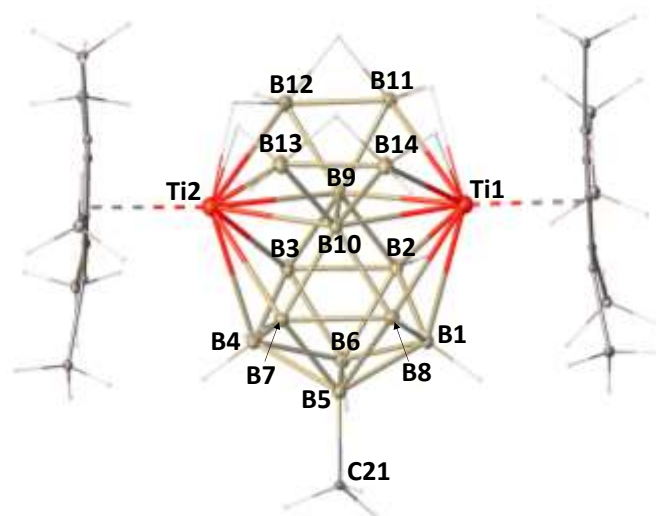


Figure S1. Molecular structure and atom labelling diagram of **2**. Selected bond lengths (\AA) and angles ($^\circ$) of **2**: Ti1-B9 2.288(5), Ti1-B10 2.308(5), Ti2-B9 2.306(5), Ti1-B14 2.516(7), Ti1-B1 2.417(6), B1-B8 1.756(8), B11-B12 1.714(9), B9-B10 1.931(8), C21-B5 1.592(8); B9-Ti1-B10 49.7(2), B10-B9-Ti1 65.7(2).

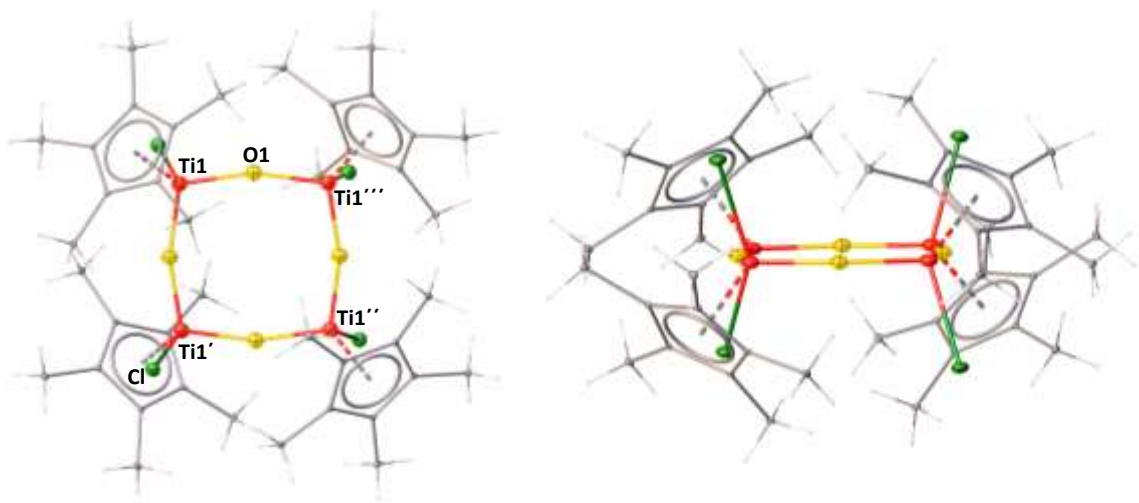


Figure S2. Molecular structure and atom labelling diagram of **3**: (left) top view; (right) side view. Selected bond lengths (\AA) and angles ($^\circ$) of **3**: Ti1-O1 1.8211(9), Ti1-Cl 2.305(2); O1-Ti1-O1 106.3(3), O1-Ti1-Cl 103.19(7).

All the spectroscopic data (*vide infra*) as well as single-crystal X-ray data revealed compound **3** as the eight-membered planar titana-oxo species $[\text{Cp}^*\text{TiCl}(\mu\text{-O})]_4$, in which four $\{\text{Cp}^*\text{TiCl}\}$ units are connected by four oxygen atoms forming the ring skeleton (Figure S2). The positions of the Cp^* group are alternating above and below the plane of this ring. Although the bromine analogue of **3**, $[\text{Cp}^*\text{TiBr}(\mu\text{-O})]_4$ has a nonplanar ring conformation, the analogue $[\text{Cp}^*\text{TiF}(\mu\text{-O})]_4$ adopts almost a planar ring conformation.⁵ Note that the formation of the titanium(IV) oxochloride complex **3** in the reaction mixture may be a result of incomplete metathesis in first instance, followed by hydrolysis or oxidation of the resultant chloride-borohydride intermediate.

I.2 Spectroscopic Details

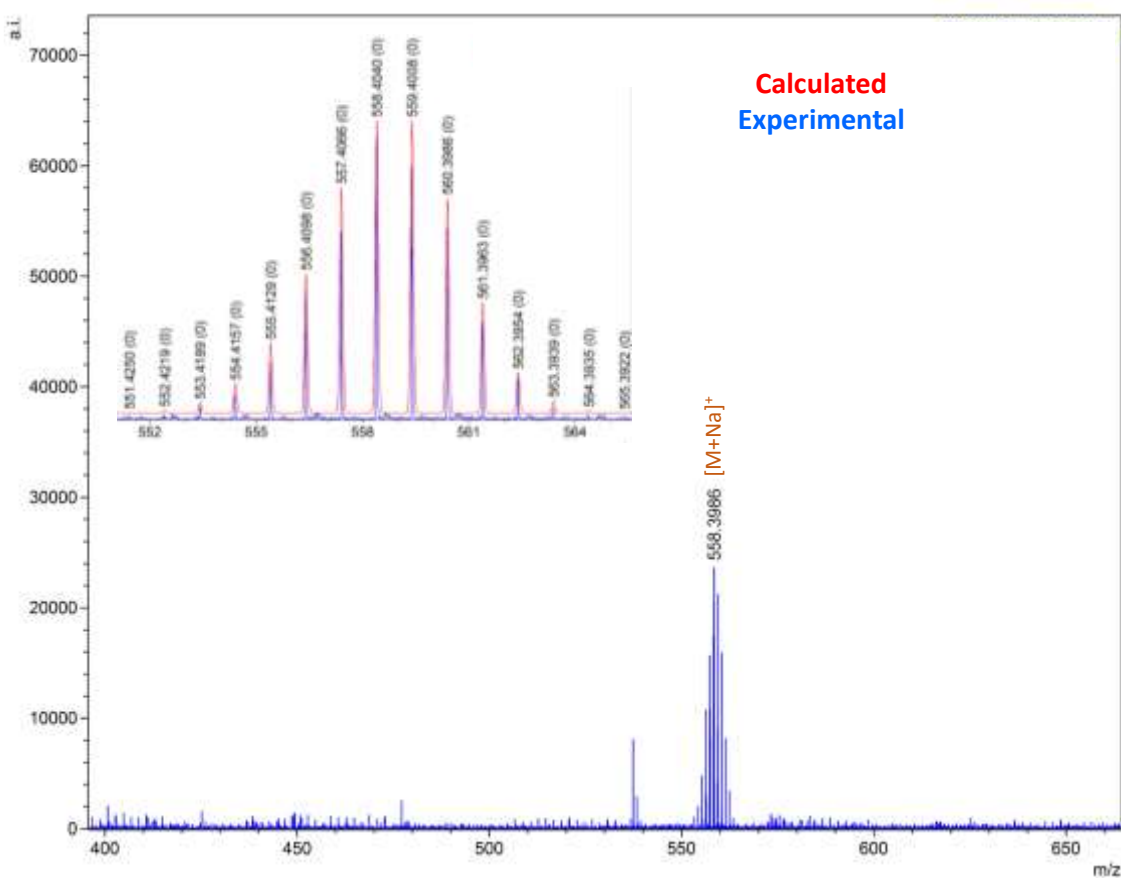


Figure S3. ESI-MS spectrum of **1**.

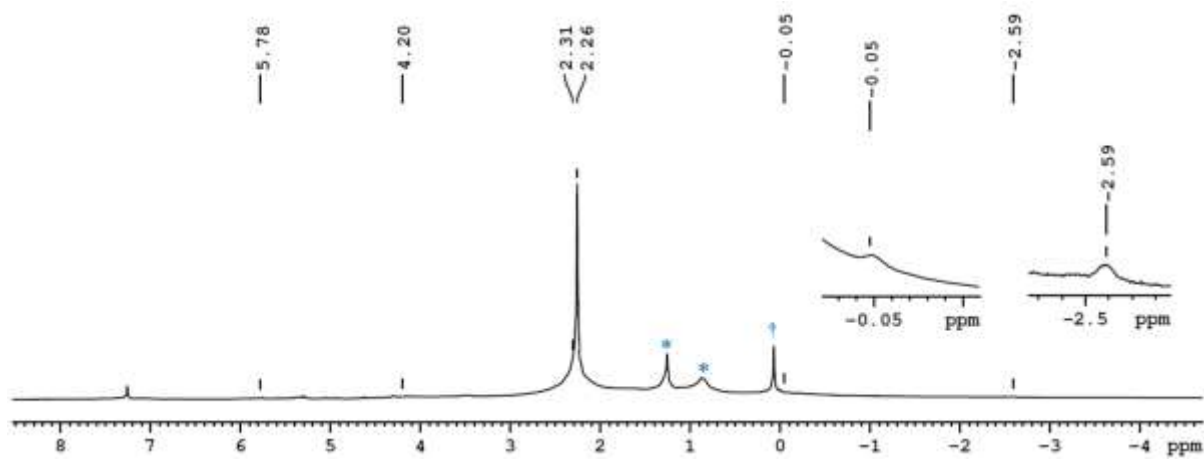


Figure S4. ^1H NMR spectrum of **1** in CDCl_3 (*Grease, †Silicon grease).

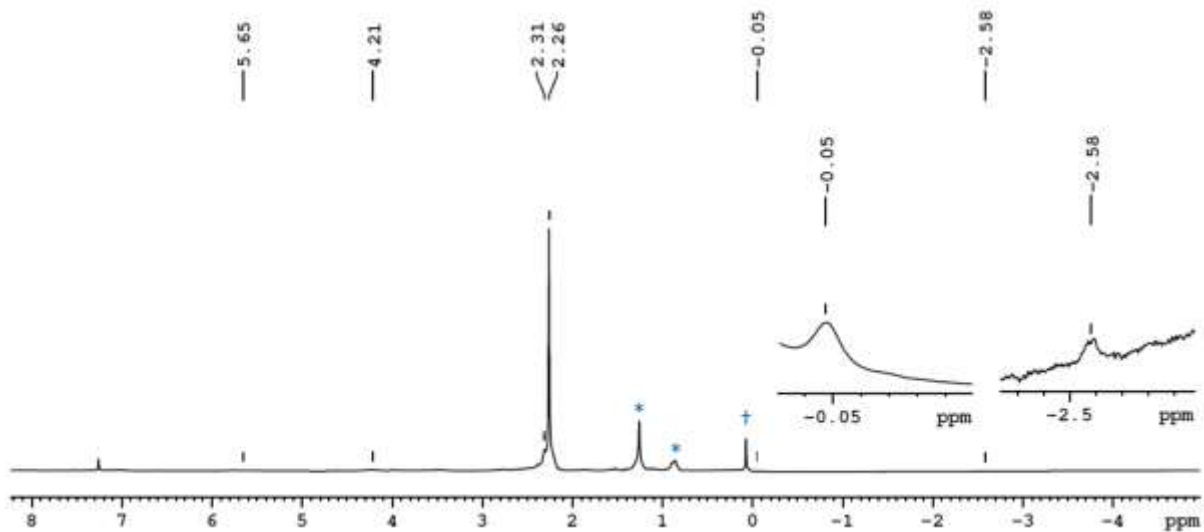


Figure S5. $^1\text{H}\{^{11}\text{B}\}$ NMR spectrum of **1** in CDCl_3 (*Grease, †Silicon grease).

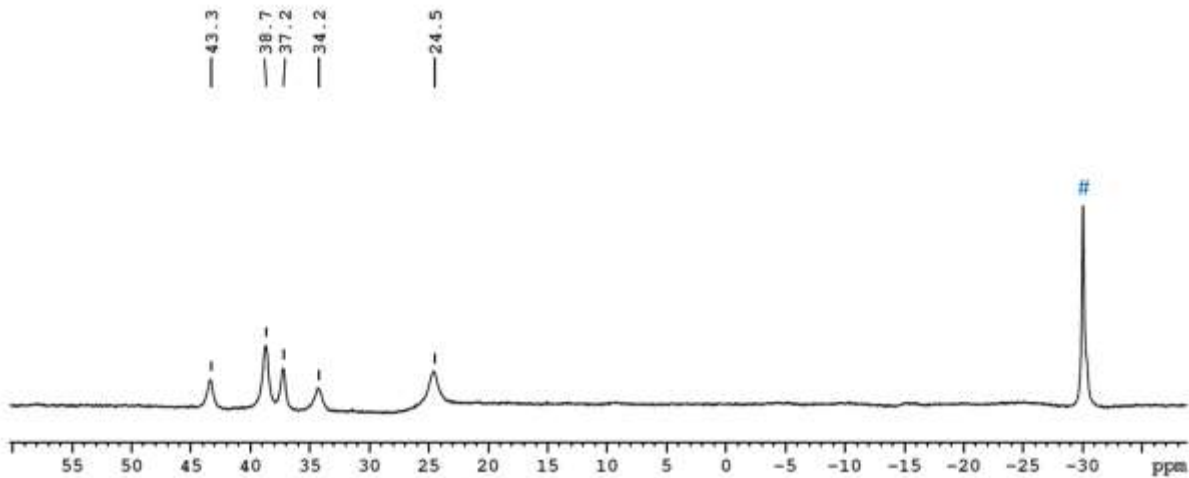


Figure S6. $^{11}\text{B}\{^1\text{H}\}$ NMR spectrum of **1** in C_6D_6 .³ (#[Bu₄N(B₃H₈)], external reference for the $^{11}\text{B}\{^1\text{H}\}$ NMR analysis)

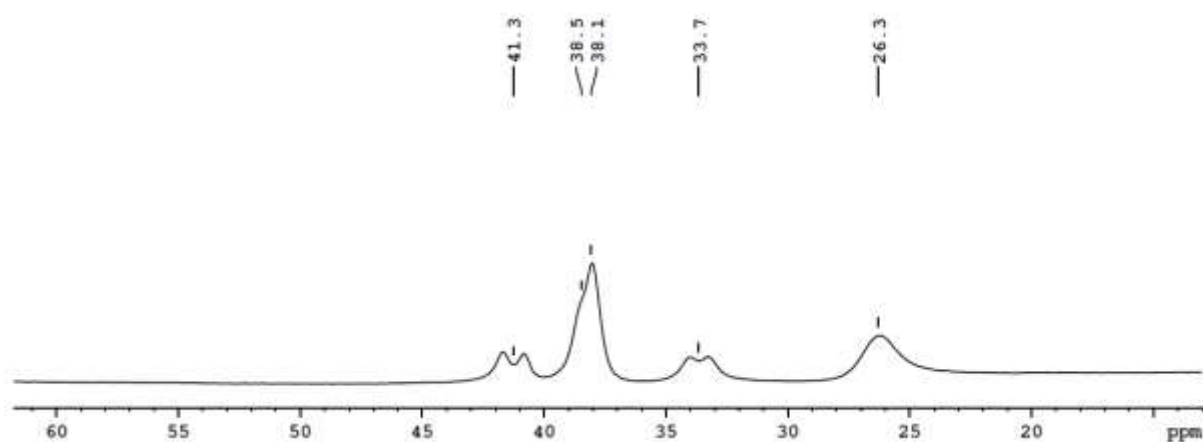


Figure S7. ^{11}B NMR spectrum of **1** in CDCl_3 .³ Note that the chemical shifts at $\delta = 38.1$ and 38.5 ppm are merged, in which one of the chemical shifts is for bare boron atoms B1 and B12 (Figure 1) and another one is for a set of four boron atoms (B4, B5, B10, and B11; Figure 1) attached to terminal hydrogens. Also, the chemical shift at $\delta = 26.3$ broadened, possibly due to the quadrupole moment of ^{11}B nuclei.

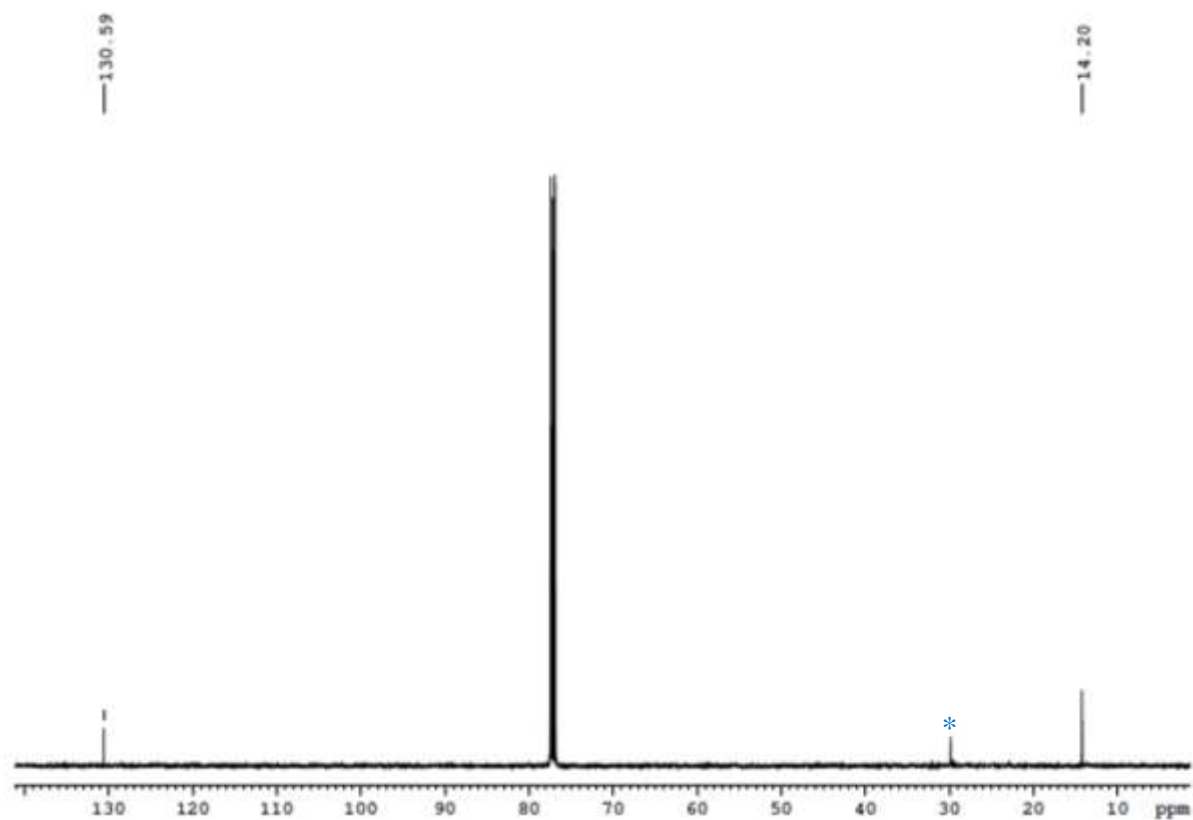


Figure S8. $^{13}\text{C}\{^1\text{H}\}$ NMR spectrum of **1** in CDCl_3 (*Grease).

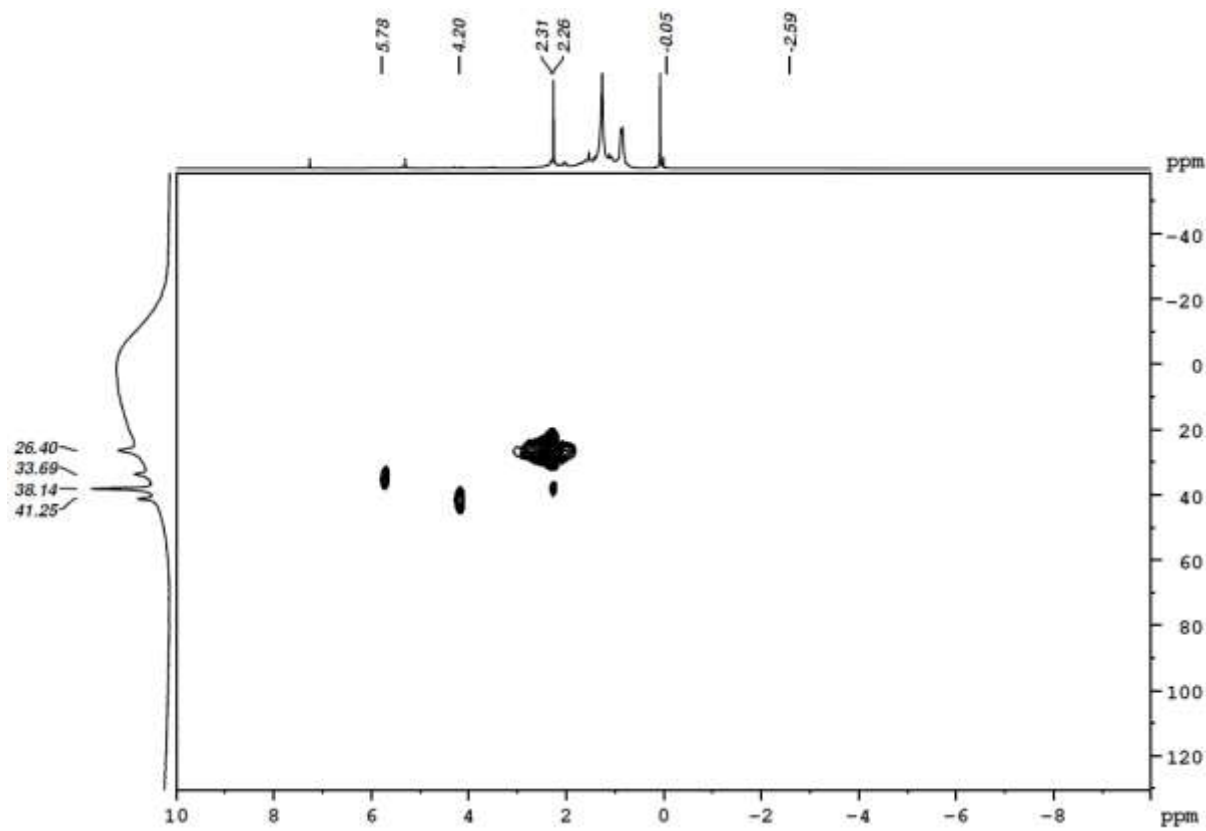


Figure S9. ^1H - ^{11}B HSQC NMR spectrum of **1** in CDCl_3 . Note that in CDCl_3 the $^{11}\text{B}\{^1\text{H}\}$ peak at 38.14 ppm for six boron atoms, which is separated in C_6D_6 in 4:2 ratio. Also, no correlation of ^1H chemical shifts at $\delta = -0.05$ and -2.59 ppm with ^{11}B chemical shifts is observed as these two ^1H signals are very weak.

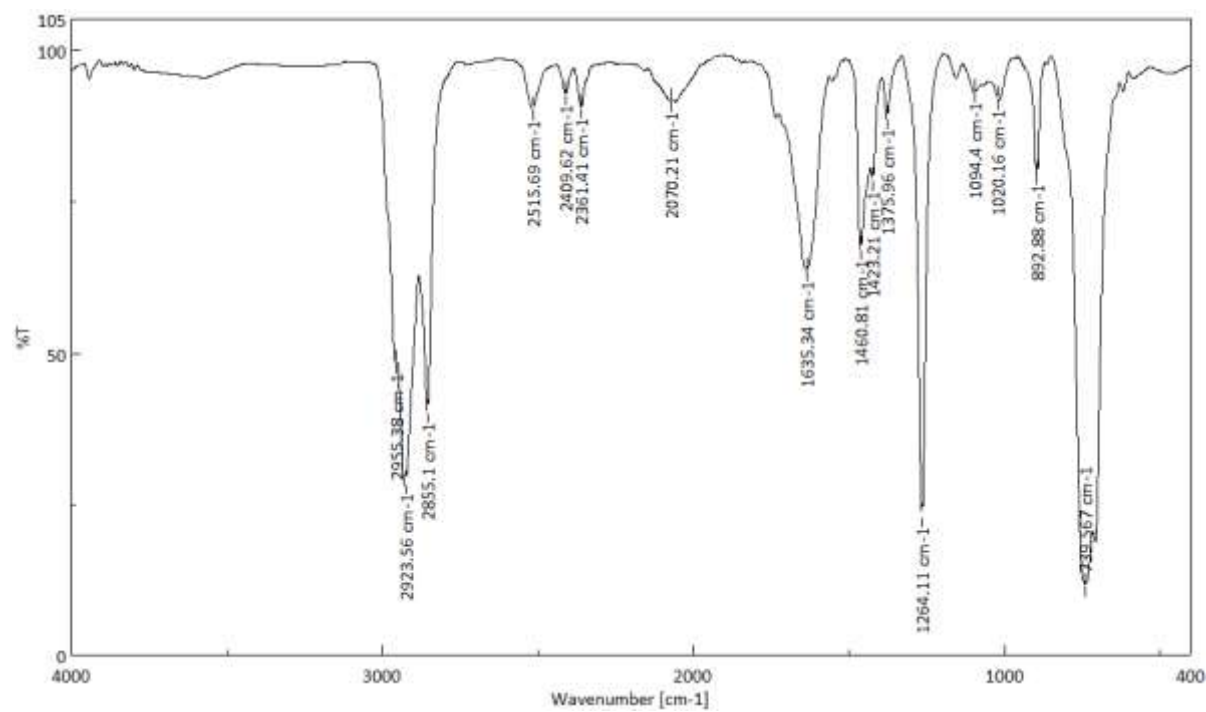


Figure S10. IR spectrum of **1**.

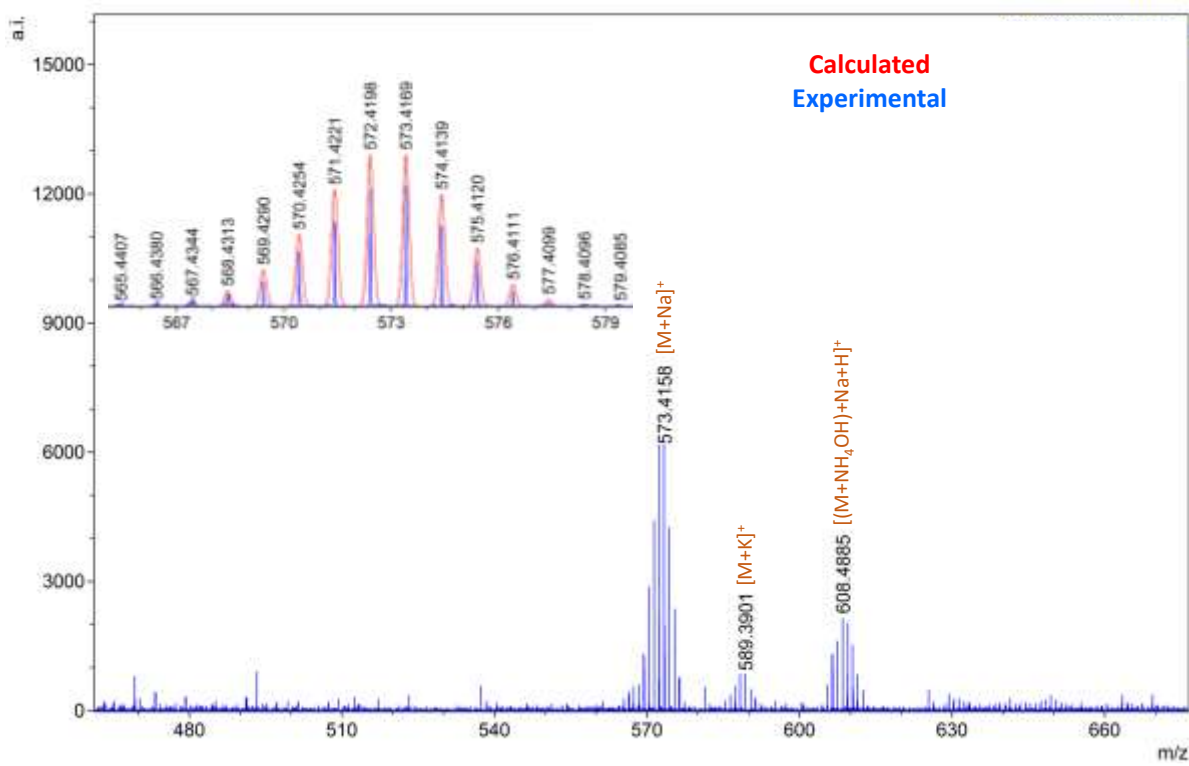


Figure S11. ESI-MS spectrum of **2**.

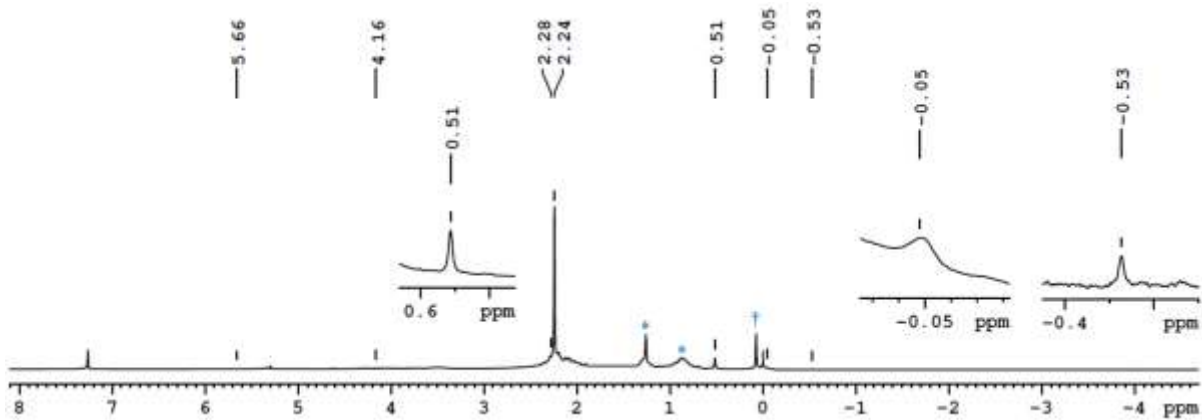


Figure S12. ^1H NMR spectrum of **2** in CDCl_3 (*Grease, †Silicon grease).

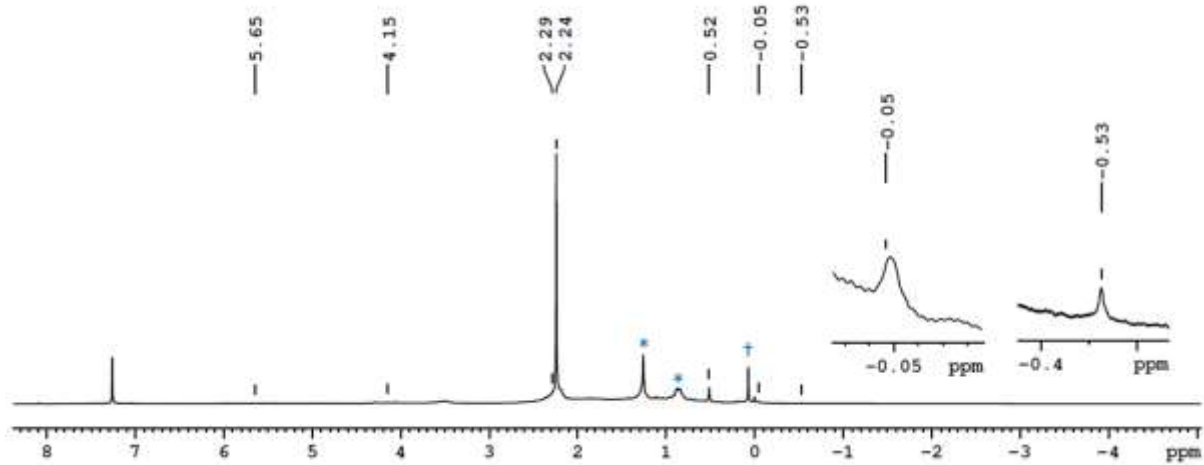


Figure S13. $^1\text{H}\{^{11}\text{B}\}$ NMR spectrum of **2** in CDCl_3 (*Grease, †Silicon grease).

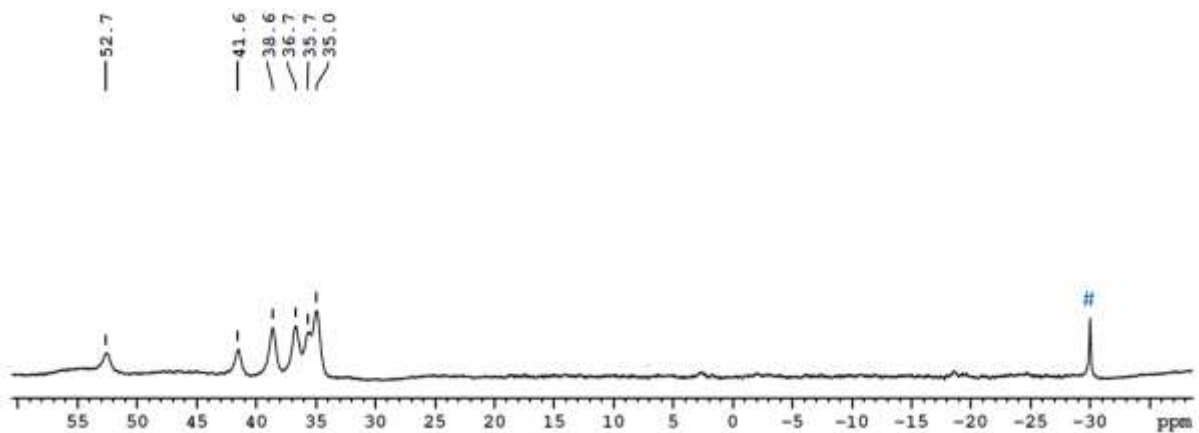


Figure S14. $^{11}\text{B}\{^1\text{H}\}$ NMR spectrum of **2** in C_6D_6 .³ (# $[\text{Bu}_4\text{N}(\text{B}_3\text{H}_8)]$, external reference for the $^{11}\text{B}\{^1\text{H}\}$ NMR analysis)

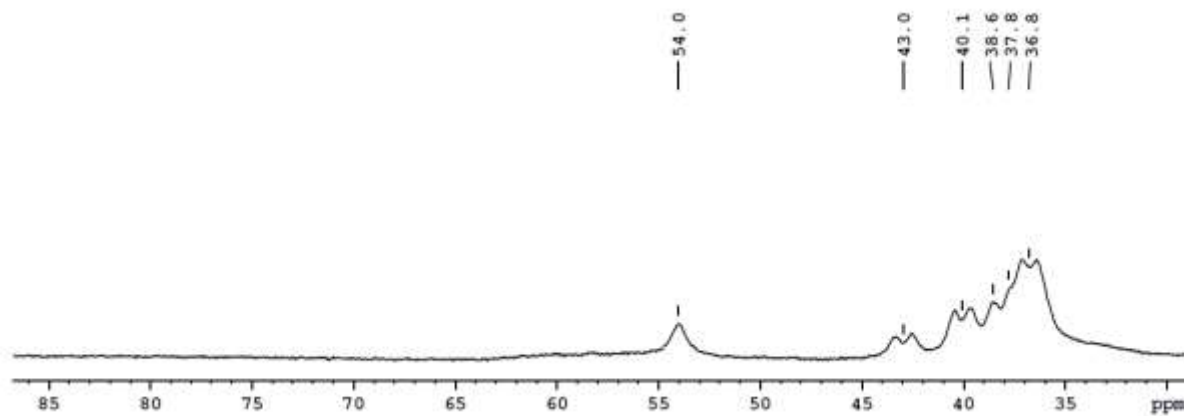


Figure S15. ^{11}B NMR spectrum of **2** in CDCl_3 .³ Note that the chemical shifts at $\delta = 54.0$ and 38.6 ppm did not show any coupling as the peak at $\delta = 54.0$ ppm corresponds to boron atom attached to methyl and the peak at $\delta = 38.6$ ppm corresponds to bare boron atoms. Also, the chemical shifts at $\delta = 37.8$ and 36.8 ppm are merged.

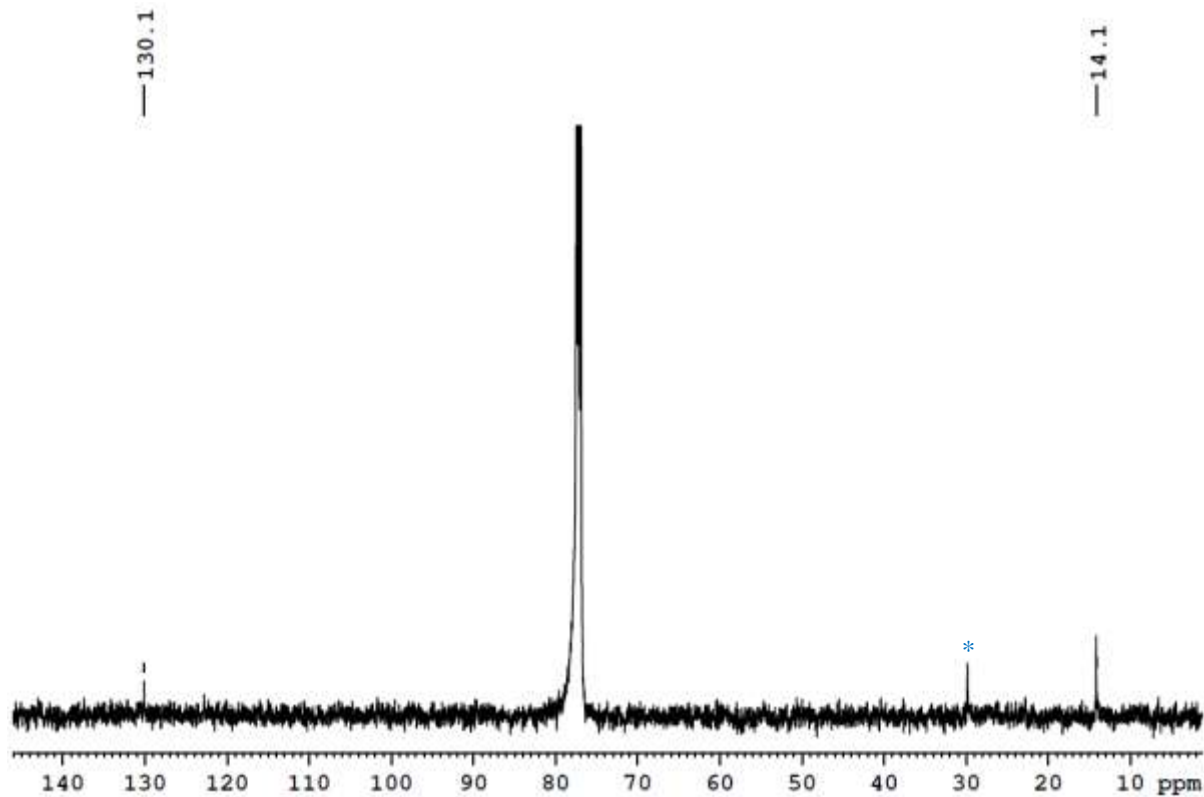


Figure S16. $^{13}\text{C}\{^1\text{H}\}$ NMR spectrum of **2** in CDCl_3 . (*Grease)

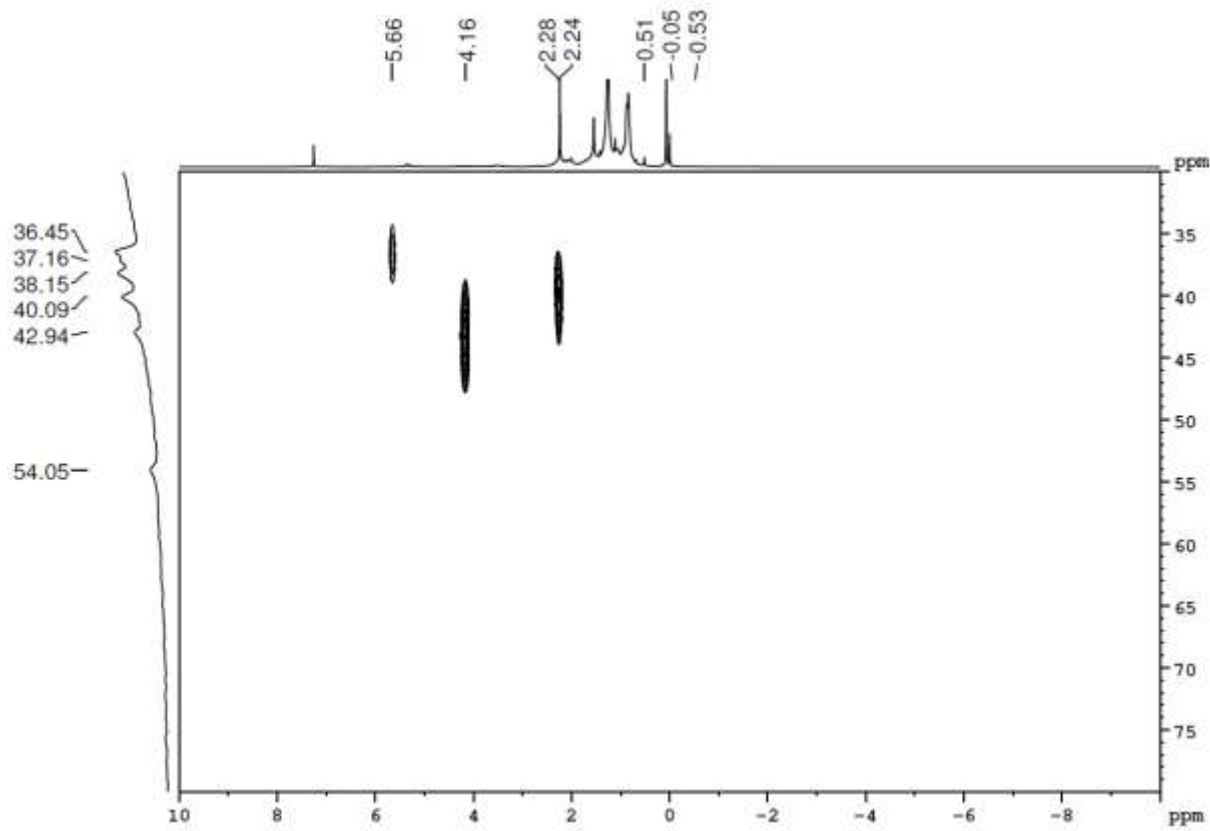


Figure S17. ^1H - ^{11}B HSQC NMR spectrum of **2** in CDCl_3 . Note that no correlation of ^1H chemical shifts at $\delta = -0.05$ and -0.53 ppm with ^{11}B chemical shifts is observed as these two ^1H signals are very weak.

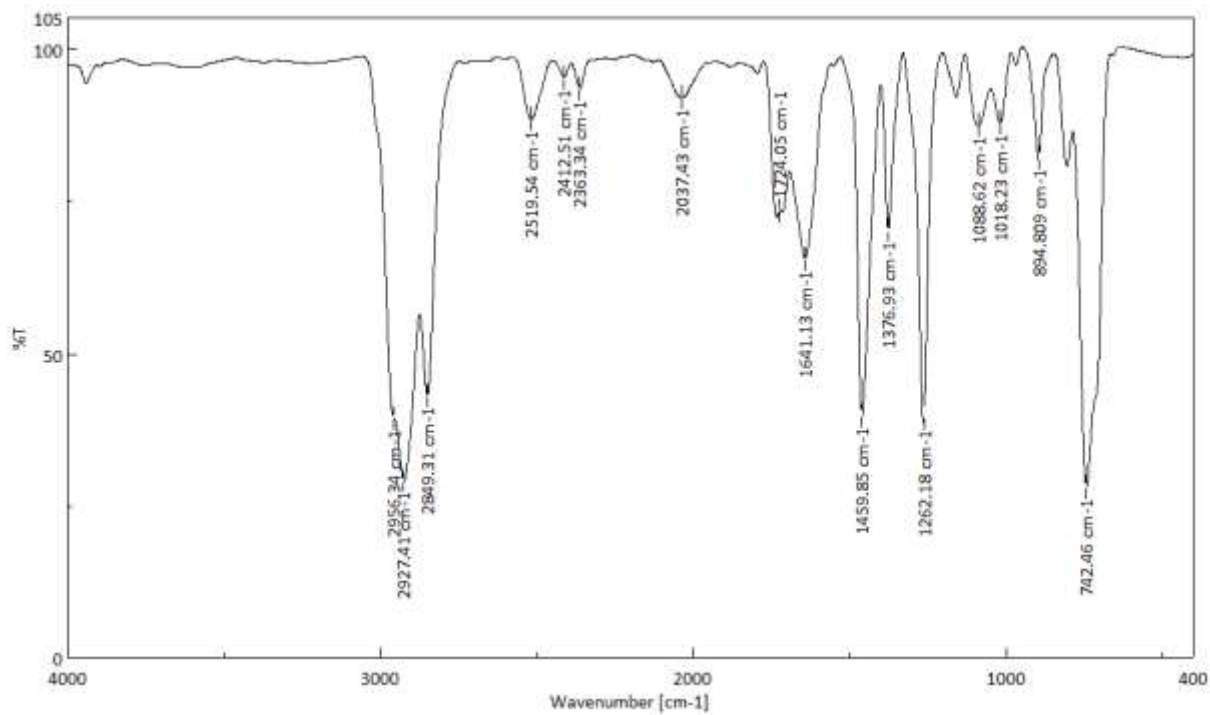


Figure S18. IR spectrum of **2**.

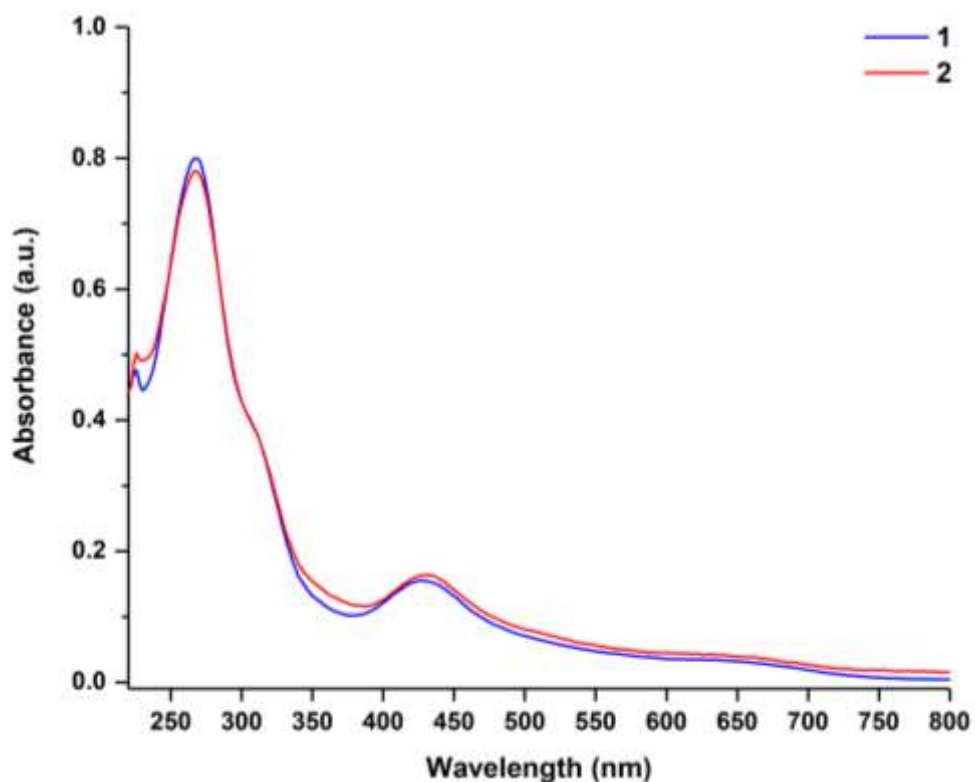


Figure S19. Combined UV-vis spectra of **1** and **2** in CH_2Cl_2 .

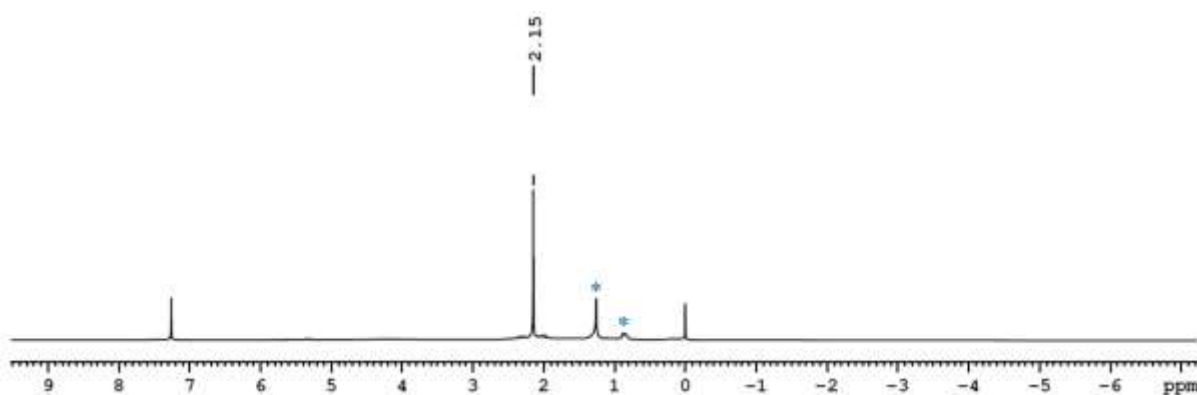


Figure S20. ^1H NMR spectrum of **3** in CDCl_3 . (*Grease)

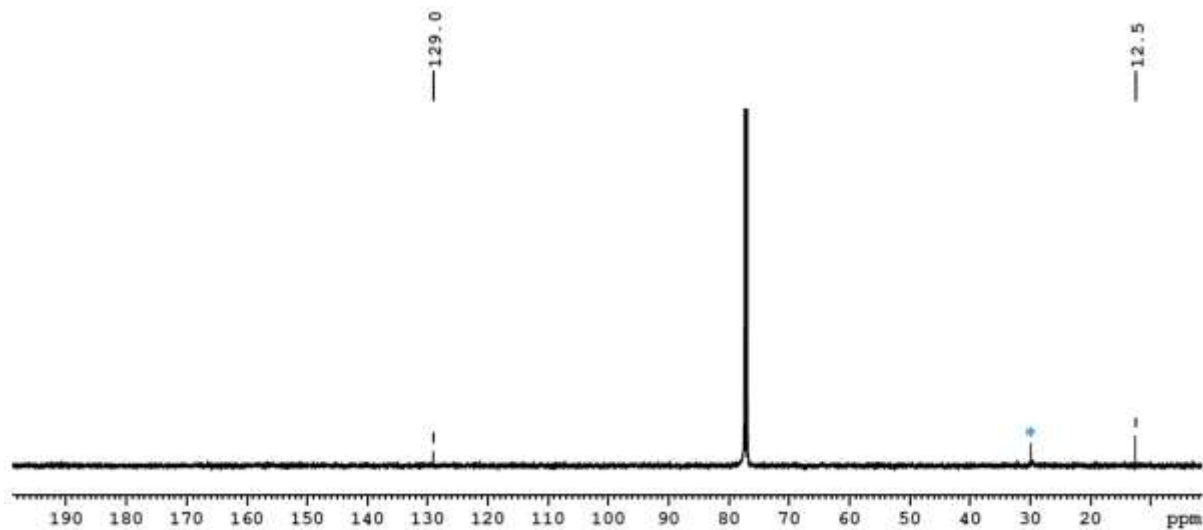


Figure S21. $^{13}\text{C}\{^1\text{H}\}$ NMR spectrum of **3** in CDCl_3 . (*Grease)

I.2 X-ray Analysis Details

Suitable X-ray quality crystals of **1**, **2** and **3** were grown by slow diffusion of a hexane-dichloromethane solution at 3 °C. Crystal data were obtained and integrated using a Bruker D8 VENTURE diffractometer with PHOTON II detector (for **1**, **2** and **3**), with graphite monochromated MoK α ($\lambda = 0.71073 \text{ \AA}$) radiation at 296 K for **1**, CuK α ($\lambda = 1.54178 \text{ \AA}$) radiation at 296 K for **2**, and CuK α ($\lambda = 1.54178 \text{ \AA}$) radiation at 297 K for **3**. The structures were solved using SIR92⁶ and refined with SHELXT-2018/2.⁷ Using Olex2⁸ the molecular structure was drawn. Crystallographic data have been deposited with the Cambridge Crystallographic Data Center as supplementary publication no CCDC-2195922 (**1**), 2257775 (**2**) and 2257779 (**3**). These data can be obtained free of charge from The Cambridge Crystallographic Data Centre via www.ccdc.cam.ac.uk/data_request/cif.

Crystal data for **1**: $\text{C}_{20}\text{H}_{48}\text{B}_{14}\text{Ti}_2$, $M_r = 535.72$, Monoclinic, space group $P2_1/n$, $a = 8.5861(3) \text{ \AA}$, $b = 33.4748(13) \text{ \AA}$, $c = 10.7145(4) \text{ \AA}$, $\alpha = 90^\circ$, $\beta = 106.9810(10)^\circ$, $\gamma = 90^\circ$, $V = 2945.28(19) \text{ \AA}^3$, $Z = 4$, $\rho_{\text{calcd}} = 1.208 \text{ g/cm}^3$, $\mu = 0.553 \text{ mm}^{-1}$, $F(000) = 1128.0$, $R_1 = 0.0726$, $wR_2 = 0.1738$, 5171 independent reflections [$2\theta \leq 49.992^\circ$] and 397 parameters.

Crystal data for **2**: $\text{C}_{21}\text{H}_{50}\text{B}_{14}\text{Ti}_2$, $M_r = 549.75$, Monoclinic, space group $P2_1/n$, $a = 10.4697(7) \text{ \AA}$, $b = 15.0305(11) \text{ \AA}$, $c = 20.0992(15) \text{ \AA}$, $\alpha = 90^\circ$, $\beta = 103.344(4)^\circ$, $\gamma = 90^\circ$, $V = 3077.5(4) \text{ \AA}^3$, $Z = 4$, $\rho_{\text{calcd}} = 1.187 \text{ g/cm}^3$, $\mu = 4.458 \text{ mm}^{-1}$, $F(000) = 1160.0$, $R_1 = 0.0645$, $wR_2 = 0.2229$, 5704 independent reflections [$2\theta \leq 139.376^\circ$] and 402 parameters.

Crystal data for **3**: $\text{C}_{40}\text{H}_{60}\text{Cl}_4\text{O}_4\text{Ti}_4$, $M_r = 938.28$, Tetragonal, space group $I-42m$, $a = 16.8466(3) \text{ \AA}$, $b = 16.8466(3) \text{ \AA}$, $c = 8.9685(3) \text{ \AA}$, $\alpha = 90^\circ$, $\beta = 90^\circ$, $\gamma = 90^\circ$, $V = 2545.33(12) \text{ \AA}^3$, $Z = 2$, $\rho_{\text{calcd}} = 1.224 \text{ g/cm}^3$, $\mu = 7.340 \text{ mm}^{-1}$, $F(000) = 976.0$, $R_1 = 0.0462$, $wR_2 = 0.1296$, 1275 independent reflections [$2\theta \leq 140.906^\circ$] and 66 parameters.

II Computational Details

All molecules were fully optimized using the *Gaussian 09*⁹ program employing the PBE1PBE functional¹⁰ in conjunction with a def2-tzvp basis set from EMSL Basis Set Exchange Library.¹¹ The model compounds were fully optimized in gaseous state (no solvent effect) starting from the X-ray crystallographic coordinates. Frequency calculations were performed at the same level of theory to verify the nature of the stationary states and the absence of any imaginary frequency to confirm that all structures represent minima on the potential energy hypersurface. Further, the gauge including atomic orbital (GIAO)¹²⁻¹⁴ method was employed to compute the ^{11}B chemical shifts. The NMR chemical shifts were calculated using the hybrid Becke–Lee–Yang–Parr (B3LYP) functional¹⁵ and the def2-TZVP basis set on the PBE1PBE/def2-TZVP optimized

geometries. The ^{11}B NMR chemical shifts were calculated relative to B_2H_6 (B3LYP B shielding constant 84.05 ppm) and converted to the usual $[\text{BF}_3\cdot\text{OEt}_2]$ scale using the experimental δ (^{11}B) value of B_2H_6 , 16.6 ppm.¹⁶ Natural bonding analyses were performed with the natural bond orbital (NBO) partitioning scheme¹⁷ as implemented in the Gaussian 09 suite of programs. Wiberg bond indexes (WBI)¹⁸ were obtained from a natural bond orbital analysis. In order to understand the nature of bonding in the synthesised molecules in greater detail, the topological properties of the resultant electron density, ρ , obtained from the wave functions of all the optimized structures were analyzed with the quantum theory of atoms in molecules (QTAIM).¹⁹ The QTAIM analysis was carried out utilizing the Multiwfn V.3.4 package²⁰ whereas the wave functions were generated with Gaussian09 at the same level of theory as for geometry optimization. All the optimized structures and orbital graphics were generated using the Gaussview²¹, and Chemcraft²² visualization programs.

Table S1. Bond parameters of $[(\text{Cp}^*\text{Ti})_2\text{B}_{14}\text{H}_{18}]$ (**1**) and $[(\text{Cp}^*\text{Ti})_2\text{B}_{14}\text{H}_{17}\text{Me}]$ (**2**) are compared with their optimized values. All distances are in Å. Θ are the dihedral angles.

$[(\text{Cp}^*\text{Ti})_2\text{B}_{14}\text{H}_{18}]$ (1)			$[(\text{Cp}^*\text{Ti})_2\text{B}_{14}\text{H}_{17}\text{Me}]$ (2)				
	Expt.	Cal.	WBI		Expt.	Cal.	WBI
Ti1-B1	2.309(5)	2.284	0.688	Ti2-B9	2.306(5)	2.283	0.456
Ti1-B12	2.300(4)	2.286	0.685	Ti2-B10	2.288(5)	2.287	0.453
Ti1-B2	2.500(5)	2.485	0.556	Ti2-B12	2.498(7)	2.481	0.299
Ti1-B14	2.490(5)	2.482	0.556	Ti2-B13	2.491(7)	2.487	0.296
Ti1-B5	2.429(5)	2.404	0.602	Ti2-B3	2.417(6)	2.401	0.404
Ti1-B11	2.422(5)	2.408	0.599	Ti2-B7	2.426(6)	2.406	0.399
Ti1-B8	2.426(5)	2.394	0.663	Ti2-B4	2.412(6)	2.391	0.466
Ti2-B1	2.299(5)	2.287	0.685	Ti1-B9	2.288(5)	2.284	0.456
Ti2-B12	2.292(5)	2.284	0.688	Ti1-B10	2.308(5)	2.288	0.453
Ti2-B3	2.503(6)	2.482	0.556	Ti1-B11	2.512(7)	2.481	0.300
Ti2-B13	2.502(5)	2.485	0.556	Ti1-B14	2.516(7)	2.486	0.296
Ti2-B4	2.437(5)	2.408	0.599	Ti1-B2	2.393(6)	2.401	0.404
Ti2-B10	2.422(5)	2.404	0.602	Ti1-B8	2.416(6)	2.406	0.399
Ti2-B7	2.435(5)	2.394	0.663	Ti1-B1	2.417(6)	2.391	0.467
B1-B12	1.926(6)	1.919	0.547	B9-B10	1.931(8)	1.919	0.471
B2-B3	1.717(8)	1.707	0.802	B11-B12	1.714(9)	1.708	0.653
B13-B14	1.716(8)	1.707	0.802	B13-B14	1.722(10)	1.707	0.655
B4-B5	1.778(7)	1.763	0.675	B2-B3	1.787(8)	1.763	0.551
B10-B11	1.796(7)	1.763	0.675	B7-B8	1.812(9)	1.759	0.555
B1-B2	1.776(7)	1.755	0.696	B9-B12	1.777(9)	1.755	0.566
B1-B3	1.781(7)	1.755	0.699	B9-B11	1.768(8)	1.755	0.566
B12-B14	1.774(7)	1.755	0.699	B10-B13	1.774(8)	1.754	0.565
B12-B13	1.772(6)	1.755	0.696	B10-B14	1.763(8)	1.754	0.565
B1-B5	1.765(6)	1.752	0.676	B3-B9	1.764(8)	1.753	0.558
B1-B4	1.757(6)	1.753	0.676	B2-B9	1.761(8)	1.753	0.558
B11-B12	1.770(6)	1.753	0.675	B7-B10	1.782(8)	1.749	0.561
B10-B12	1.772(6)	1.752	0.676	B8-B10	1.767(8)	1.749	0.560
B5-B6	1.776(7)	1.762	0.650	B3-B6	1.755(10)	1.759	0.533
B5-B8	1.783(7)	1.773	0.671	B3-B4	1.753(9)	1.772	0.588
B8-B11	1.777(7)	1.773	0.671	B4-B7	1.764(9)	1.771	0.589
B9-B11	1.785(7)	1.763	0.649	B5-B7	1.763(8)	1.776	0.518
B6-B8	1.788(7)	1.781	0.635	B4-B6	1.758(9)	1.778	0.511
B8-B9	1.797(7)	1.781	0.634	B4-B5	1.799(9)	1.795	0.497
B6-B9	1.765(8)	1.765	0.636	B5-B6	1.795(10)	1.776	0.521
B6-B7	1.789(7)	1.782	0.634	B1-B6	1.771(9)	1.779	0.510
B7-B9	1.787(7)	1.781	0.635	B1-B5	1.789(8)	1.794	0.497
B7-B10	1.776(7)	1.773	0.671	B1-B8	1.756(8)	1.770	0.590
B4-B7	1.785(7)	1.773	0.671	B1-B2	1.778(9)	1.772	0.588
Θ (Ti1-B1-B12-Ti2)	175.7(2)°	176.7°	-	B5-C21	1.592(8)	1.590	0.965
Θ (Ti1-B9-B10-Ti2)				Θ (Ti1-B9-B10-Ti2)	176.4(2)°	176.9°	-

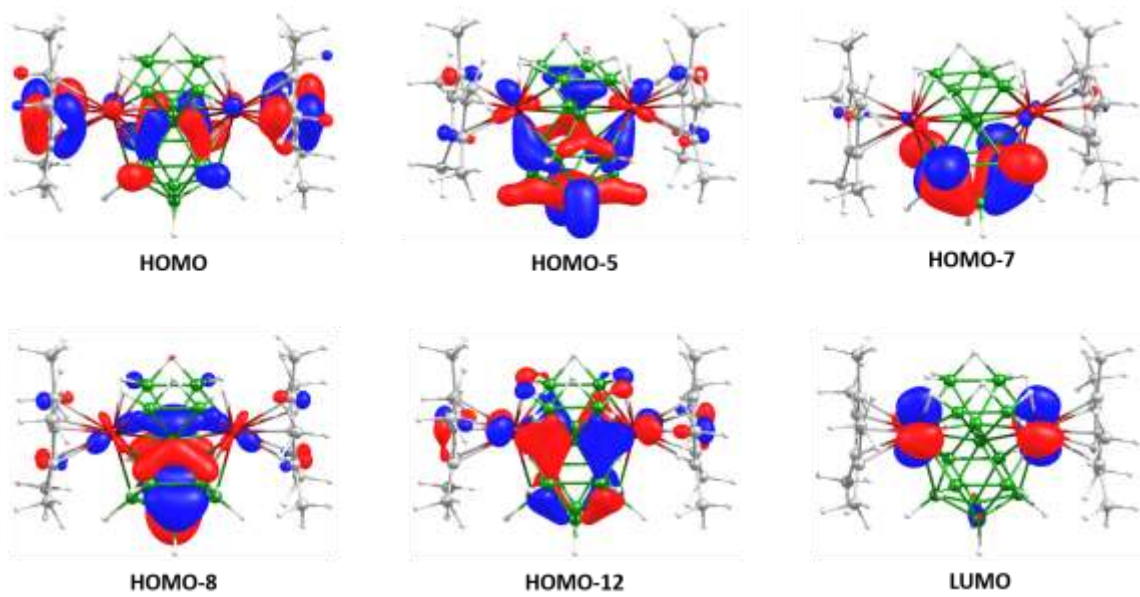


Figure S22. Selected molecular orbitals of **1** (isocontour values: ± 0.043 [e.bohr $^{-3}$] $^{1/2}$).

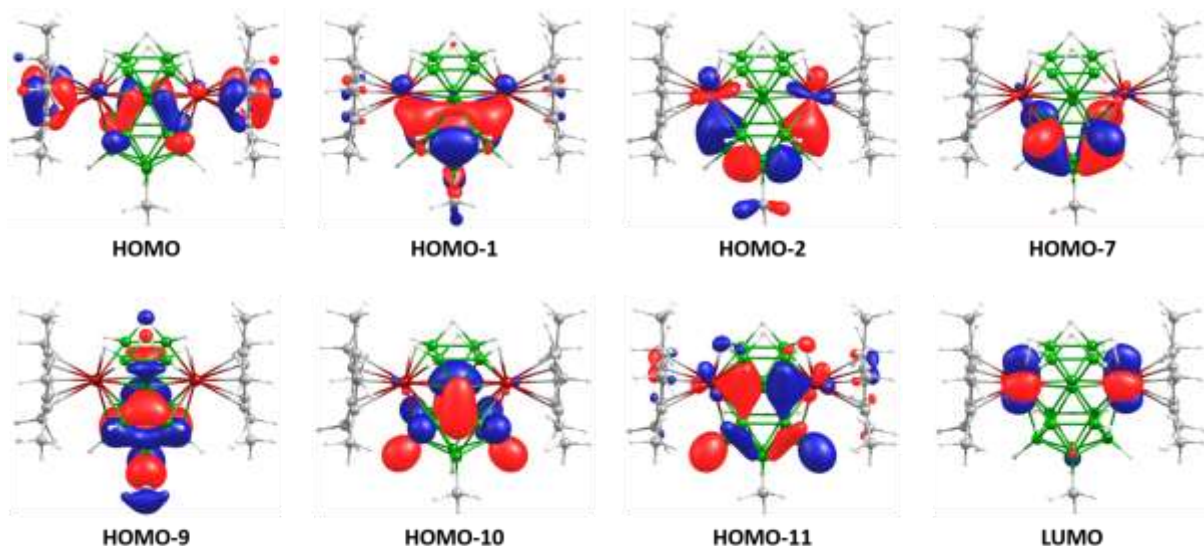


Figure S23. Selected molecular orbitals of **2** (isocontour values: ± 0.043 [e.bohr $^{-3}$] $^{1/2}$).

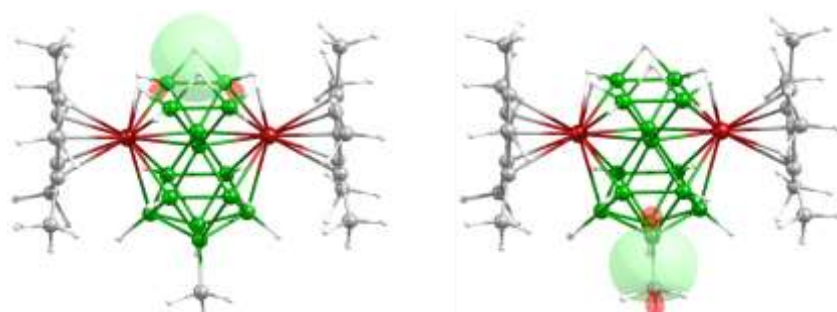


Figure S24. B–H–B (left) and B–Me (right) interactions in **2**, obtained from an NBO analysis (isocontour values: ± 0.043 [e.bohr $^{-3}$] $^{1/2}$).

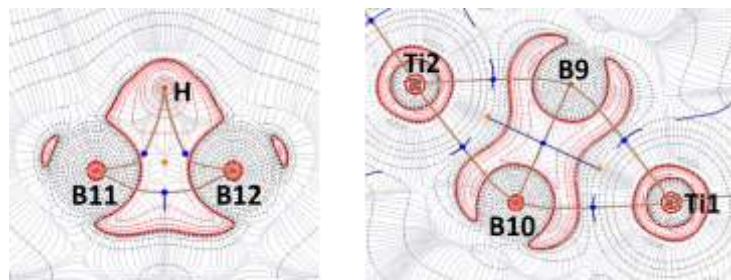


Figure S25. Contour-line diagram of the Laplacian of the electron density of **2** in the B11–H–B12 (left) and Ti1–B9–B10–Ti2 (right) planes. The solid brown lines are bond paths, whereas blue dots indicate the bond-critical points (BCP). Solid red lines indicate the areas of charge concentration ($\nabla^2\rho(r) < 0$), while dashed black lines show the areas of charge depletion ($\nabla^2\rho(r) > 0$).

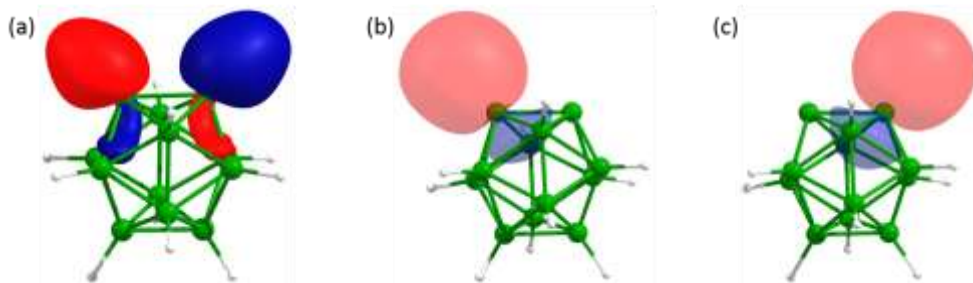


Figure S26. (a) HOMO of $[B_{12}H_{10}]^{4-}$ depicting localized orbitals on two adjacent bare boron atoms (isocontour values: $\pm 0.043 \text{ [e.bohr}^{-3}\text{]}^{1/2}$); (b) and (c) NBO analysis of $[B_{12}H_{10}]^{4-}$ depicted lone pairs on two adjacent bare boron atoms.

Table S2. Calculated natural charges (q_{Ti} , and q_{B}), natural valence populations (Pop) and HOMO–LUMO gaps ($\Delta E_{\text{H-L}}$) of **1** and **2**.

Compound	q_{Ti}	q_{B}	$\text{Pop} (\text{Ti}_{\text{val}})$	$\text{Pop} (\text{B}_{\text{val}})$	$\Delta E_{\text{H-L}} (\text{eV})$
1	0.391	-0.245	3.506	3.217	3.455
	0.391	-0.251	3.506	3.223	
		-0.181		3.152	
		-0.219		3.184	
		-0.215		3.179	
		-0.184		3.147	
		-0.204		3.167	
		-0.184		3.147	
		-0.204		3.167	
		-0.215		3.179	
		-0.219		3.184	
		-0.181		3.151	
		-0.251		3.223	
		-0.245		3.217	
2	0.392	-0.205	3.505	3.167	3.460
	0.392	-0.219	3.505	3.184	
		-0.220		3.185	
		-0.203		3.166	
		-0.195		3.156	
		-0.219		3.183	
		-0.217		3.180	
		-0.187		3.158	
		-0.179		3.149	
		-0.246		3.219	
		-0.246		3.219	
		-0.249		3.221	
		-0.249		3.221	
		0.097 ^[a]		2.864 ^[a]	

^[a]Data is for B5 attached to methyl group in compound **2**.

III Cartesian Coordinates of all Optimized Structures

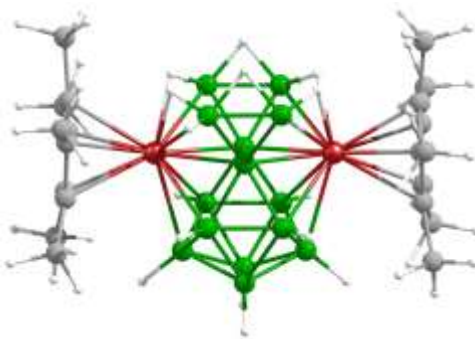


Figure S27. Optimized geometry of **1**.

Total energy = -2836.73489769 a.u.

Cartesian coordinates for the calculated structure **1** (in Å)

C	-4.154998000000	0.695467000000	-0.795999000000	C	4.386920000000	2.062072000000	-1.414586000000
C	-4.120077000000	-0.686347000000	-1.109673000000	H	4.435537000000	2.940142000000	-0.773806000000
C	-4.082435000000	-1.419629000000	0.109620000000	H	3.597608000000	2.231849000000	-2.149475000000
C	-4.107006000000	-0.480324000000	1.178105000000	H	5.337697000000	1.981155000000	-1.952141000000
C	-4.155338000000	0.821148000000	0.624317000000	C	4.197065000000	-0.786828000000	-2.633193000000
C	-4.355795000000	1.797724000000	-1.776258000000	H	3.823586000000	-1.783171000000	-2.869021000000
H	-3.966812000000	1.536234000000	-2.760352000000	H	5.241172000000	-0.737810000000	-2.961791000000
H	-3.857089000000	2.712251000000	-1.457689000000	H	3.631477000000	-0.067251000000	-3.227408000000
H	-5.425171000000	2.009436000000	-1.885314000000	B	-0.840495000000	-1.454816000000	-1.782257000000
C	-4.221809000000	-1.266772000000	-2.479732000000	B	0.866019000000	-1.466005000000	-1.759395000000
H	-3.825751000000	-2.281645000000	-2.523542000000	B	0.009766000000	-0.158501000000	-0.960369000000
H	-3.681703000000	-0.669042000000	-3.214985000000	B	-0.866986000000	1.267685000000	-1.481020000000
H	-5.270461000000	-1.306585000000	-2.793258000000	H	-1.481276000000	1.283293000000	-2.510352000000
C	-4.176418000000	-2.903858000000	0.241414000000	B	0.895944000000	1.266841000000	-1.461883000000
H	-5.224560000000	-3.220648000000	0.223189000000	H	1.532432000000	1.280816000000	-2.479383000000
H	-3.746290000000	-3.256343000000	1.179932000000	B	0.009411000000	2.675262000000	-0.882103000000
H	-3.668166000000	-3.421728000000	-0.573905000000	H	0.015908000000	3.701657000000	-1.488577000000
C	-4.194617000000	-0.785939000000	2.634508000000	B	1.432248000000	2.088677000000	0.015274000000
H	-3.627998000000	-0.066586000000	3.228022000000	H	2.369371000000	2.820916000000	0.025859000000
H	-3.821481000000	-1.782442000000	2.870178000000	B	-0.009293000000	2.674557000000	0.882946000000
H	-5.238381000000	-0.736251000000	2.964077000000	H	-0.015824000000	3.700455000000	1.490254000000
C	-4.386378000000	2.062469000000	1.414757000000	B	-1.432097000000	2.088623000000	-0.014903000000
H	-5.338482000000	1.982773000000	1.950171000000	H	-2.369258000000	2.820798000000	-0.025192000000
H	-4.432297000000	2.940709000000	0.774032000000	B	-0.895965000000	1.265612000000	1.461643000000
H	-3.598466000000	2.230955000000	2.151441000000	H	-1.532046000000	1.278885000000	2.479378000000
C	4.082601000000	-1.419608000000	-0.108120000000	B	0.867103000000	1.266420000000	1.480789000000
C	4.119026000000	-0.685758000000	1.110895000000	H	1.480975000000	1.281369000000	2.510343000000
C	4.154211000000	0.695894000000	0.796674000000	B	-0.009686000000	-0.159246000000	0.958899000000
C	4.155833000000	0.821012000000	-0.623670000000	B	-0.865967000000	-1.467517000000	1.756687000000
C	4.108242000000	-0.480778000000	-1.176944000000	B	0.840578000000	-1.456298000000	1.779511000000
C	4.176803000000	-2.903884000000	-0.239196000000	Ti	-2.073331000000	-0.217613000000	-0.019397000000
H	3.747922000000	-3.256748000000	-1.178147000000	Ti	2.073347000000	-0.217797000000	0.017500000000
H	3.667505000000	-3.421455000000	0.575660000000	H	0.007627000000	-2.499697000000	-1.740664000000
H	5.224926000000	-3.220649000000	-0.219477000000	H	1.332078000000	-1.395305000000	-2.853287000000
C	4.219570000000	-1.265637000000	2.481253000000	H	-1.276817000000	-1.377647000000	-2.887911000000
H	3.822666000000	-2.280164000000	2.525320000000	H	-1.699860000000	-1.893806000000	0.940081000000
H	3.679533000000	-0.667088000000	3.215886000000	H	1.703431000000	-1.880949000000	0.990367000000
H	5.268031000000	-1.306134000000	2.795342000000	H	1.276259000000	-1.380489000000	2.885494000000
C	4.354267000000	1.798252000000	1.776946000000	H	-1.331476000000	-1.398084000000	2.850881000000
H	5.423761000000	2.007531000000	1.889431000000	H	-0.007567000000	-2.501228000000	1.736391000000
H	3.961335000000	1.538233000000	2.759867000000	H	-1.703076000000	-1.880288000000	-0.993273000000
H	3.858622000000	2.713699000000	1.456310000000	H	1.699592000000	-1.893450000000	-0.943004000000

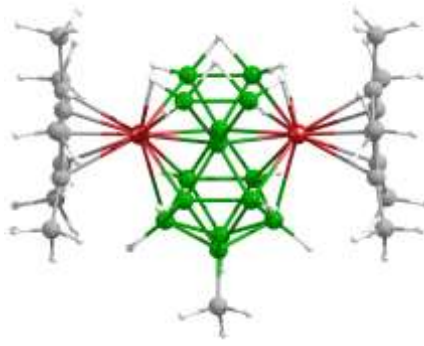


Figure S28. Optimized geometry of **2**

Total energy = -2876.02374292 a.u.

Cartesian coordinates for the calculated structure **2** (in Å)

Ti	-2.073656000000	-0.338060000000	0.023732000000	C	4.383453000000	2.230718000000	0.838945000000
Ti	2.073520000000	-0.337735000000	0.024688000000	H	4.377803000000	2.924131000000	0.000674000000
C	-4.161504000000	0.345830000000	-0.950004000000	H	3.623001000000	2.561511000000	1.548614000000
C	-4.154152000000	0.829321000000	0.391125000000	H	5.358708000000	2.302360000000	1.332573000000
C	-4.101399000000	-0.287801000000	1.258408000000	C	4.182220000000	-0.216081000000	2.745083000000
C	-4.080264000000	-1.468568000000	0.464272000000	H	3.810874000000	-1.122740000000	3.222633000000
C	-4.125235000000	-1.070219000000	-0.901219000000	H	5.223833000000	-0.080356000000	3.056666000000
C	-4.235162000000	-1.979201000000	-2.078550000000	H	3.609967000000	0.626596000000	3.136660000000
H	-3.693459000000	-1.592689000000	-2.942857000000	C	0.000581000000	4.247560000000	0.502594000000
H	-3.847492000000	-2.975313000000	-1.863846000000	H	-0.102763000000	4.894388000000	-0.373023000000
H	-5.285291000000	-2.088466000000	-2.369929000000	H	-0.820498000000	4.485354000000	1.185721000000
C	-4.169719000000	-2.870096000000	0.971086000000	H	0.929576000000	4.528384000000	1.008310000000
H	-3.719692000000	-2.974796000000	1.959387000000	B	-1.430709000000	1.879503000000	-0.597711000000
H	-5.217539000000	-3.177107000000	1.055831000000	B	-0.881261000000	0.688402000000	-1.789416000000
H	-3.677814000000	-3.579738000000	0.303587000000	B	0.882108000000	0.688005000000	-1.789546000000
C	-4.181804000000	-0.214377000000	2.745227000000	B	1.430890000000	1.879286000000	-0.598014000000
H	-3.810474000000	-1.120802000000	3.223226000000	B	0.000067000000	2.709995000000	0.097177000000
H	-3.609521000000	0.628488000000	3.136346000000	B	0.000449000000	2.199447000000	-1.604060000000
H	-5.223410000000	-0.078469000000	3.056756000000	B	0.879890000000	1.488163000000	1.038885000000
C	-4.383089000000	2.231462000000	0.837872000000	B	-0.879917000000	1.487938000000	1.038793000000
H	-4.376978000000	2.924560000000	-0.000640000000	B	0.000183000000	-0.545604000000	-0.909465000000
H	-5.358497000000	2.303470000000	1.331155000000	B	-0.000031000000	-0.019974000000	0.936216000000
H	-3.622788000000	2.562445000000	1.547589000000	B	-0.853936000000	-2.019223000000	-1.333520000000
C	-4.373263000000	1.159097000000	-2.178767000000	B	0.854184000000	-2.019396000000	-1.332977000000
H	-3.992299000000	0.652255000000	-3.065326000000	B	0.852892000000	-1.050939000000	2.070601000000
H	-5.444061000000	1.335452000000	-2.329068000000	B	-0.853780000000	-1.050785000000	2.069792000000
H	-3.873862000000	2.124761000000	-2.112097000000	H	-0.000447000000	-2.059752000000	2.325249000000
C	4.124658000000	-1.070040000000	-0.901809000000	H	1.304809000000	-0.681886000000	3.108823000000
C	4.161216000000	0.346020000000	-0.949898000000	H	-1.306775000000	-0.682037000000	3.107644000000
C	4.154341000000	0.828816000000	0.391489000000	H	-1.697149000000	-1.678919000000	1.408709000000
C	4.101747000000	-0.288752000000	1.258226000000	H	1.696951000000	-1.678801000000	1.410282000000
C	4.080112000000	-1.469083000000	0.463485000000	H	-0.000138000000	-3.012058000000	-1.023717000000
C	4.169303000000	-2.870920000000	0.969501000000	H	-1.703363000000	-2.210063000000	-0.445743000000
H	3.719910000000	-2.975955000000	1.958054000000	H	-1.304749000000	-2.247078000000	-2.412288000000
H	3.676636000000	-3.579991000000	0.301955000000	H	1.305709000000	-2.247676000000	-2.411334000000
H	5.217045000000	-3.178440000000	1.053359000000	H	1.702650000000	-2.210225000000	-0.444338000000
C	4.234171000000	-1.978448000000	-2.079607000000	H	1.505369000000	0.424072000000	-2.779520000000
H	3.846001000000	-2.974481000000	-1.865452000000	H	-0.000256000000	3.029227000000	-2.461478000000
H	3.692681000000	-1.591184000000	-2.943706000000	H	-1.505484000000	0.424559000000	-2.778863000000
H	5.284263000000	-2.088078000000	-2.370993000000	H	-2.364312000000	2.591135000000	-0.795961000000
C	4.373107000000	1.159838000000	-2.178266000000	H	1.498213000000	1.790019000000	2.022880000000
H	3.873935000000	2.125585000000	-2.111150000000	H	-1.497519000000	1.790737000000	2.022882000000
H	5.443949000000	1.336010000000	-2.328481000000	H	2.364665000000	2.591065000000	-0.794877000000
H	3.992006000000	0.653496000000	-3.065045000000				



Figure S29. Optimized geometry of $[B_{12}H_{10}]^{4-}$.

Total energy = -303.38535783 a.u.

Cartesian coordinates for the calculated structure $[B_{12}H_{10}]^{4-}$ (in Å)

B	0.000019000000	0.593502000000	-1.695235000000	B	-1.431286000000	0.165484000000	0.815637000000
B	-0.882014000000	1.402604000000	-0.345358000000	H	-2.480548000000	0.284412000000	1.444207000000
H	-1.554465000000	2.427090000000	-0.465253000000	B	-0.881814000000	-1.430171000000	0.196103000000
B	0.881601000000	1.402858000000	-0.345239000000	H	-1.549919000000	-2.419096000000	0.479656000000
H	1.553613000000	2.427613000000	-0.465259000000	B	0.882200000000	-1.429918000000	0.196197000000
B	-0.000293000000	1.154795000000	1.199563000000	H	1.550625000000	-2.418620000000	0.479818000000
H	-0.000311000000	2.001187000000	2.094375000000	B	0.000264000000	-1.237981000000	-1.394576000000
B	1.431143000000	0.165931000000	0.815808000000	B	1.417072000000	-0.190879000000	-0.952788000000
H	2.480339000000	0.285086000000	1.444448000000	B	-1.416882000000	-0.191355000000	-0.952885000000
B	0.000054000000	-0.596979000000	1.522628000000	H	2.522460000000	-0.287667000000	-1.486548000000
H	0.000054000000	-1.051019000000	2.662061000000	H	-2.522178000000	-0.288441000000	-1.486768000000



Figure S30. Optimized geometry of $[B_{12}H_{10}]^{2-}$.

Total energy = -304.0700857 a.u.

Cartesian coordinates for the calculated structure $[B_{12}H_{10}]^{2-}$ (in Å)

B	0.000021000002	0.593502040390	-1.695235123696	B	-1.431285105008	0.165488011960	0.815637060249
B	-0.882010063932	1.402606100577	-0.345358024891	H	-2.480547178972	0.284418020522	1.444207105419
H	-1.554459110873	2.427094175410	-0.465253033675	B	-0.881818062551	-1.430169101941	0.196103014003
B	0.881605063416	1.402856099785	-0.345239025098	H	-1.549925109620	-2.419092174013	0.479656034514
H	1.553619110783	2.427609176000	-0.465259033486	B	0.882196064443	-1.429920102878	0.196197013874
B	-0.000290000021	1.154795083091	1.199563086765	H	1.550619109707	-2.418624174946	0.479818034720
H	-0.000306000022	2.001187141869	2.094375149583	B	0.000261000019	-1.237981090454	-1.394576100412
B	1.431144100438	0.165927012114	0.815808058585	B	1.417072102614	-0.190883013823	-0.952788066038
H	2.480340180708	0.285080020731	1.444448103321	B	-1.416882101523	-0.191351013949	-0.952885069520
B	0.000053000004	-0.596979041839	1.522628109784	H	2.522459181283	-0.287674020618	-1.486548106433
H	0.000051000004	-1.051019074725	2.662061193212	H	-2.522179183017	-0.288434020749	-1.486768106583

References

- 1 G. H. Llinás, M. Mena, F. Palacios, P. Royo and R. Serrano, *J. Organomet. Chem.*, 1988, **340**, 37–40.
- 2 G. E. Ryschlewitsch, K. C. Nainan, S. R. Miller, L. J. Todd, W. J. Dewkett, M. Grace, H. Beall, M. F. Hawthorne and R. Leyden, *Inorg. Synth.*, 2007, **15**, 111–118.
- 3 (a) J. J. Led and H. Gesmar, *Chem. Rev.*, 1991, **91**, 1413–1426; (b) L. Yang, R. Simionescu, A. Lough and H. Yan, *Dyes Pigm.*, 2011, **91**, 264–267; (c) R. Weiss and R. N. Grimes, *J. Am. Chem. Soc.*, 1978, **100**, 1401–1405.
- 4 S. Kar, S. Bairagi, A. Haridas, G. Joshi, E. D. Jemmis and S. Ghosh, *Angew. Chem. Int. Ed.*, 2022, **61**, e202208293.
- 5 (a) H. W. Roesky, I. Leichtweis and M. Noltemeyer, *Inorg. Chem.*, 1993, **32**, 5102–5104; (b) F. Palacios, P. Royo, R. Serrano, J. L. Balcázar, I. Fonseca, F. Florencio, *J. Organomet. Chem.*, 1989, **375**, 51–58.
- 6 A. Altomare, G. Cascarano, C. Giacovazzo, A. Guagliardi, M. C. Burla, G. Polidori and M. Camalli, *J. Appl. Crystallogr.*, 1994, **27**, 435–436.
- 7 G. M. Sheldrick, *Acta Cryst.*, 2015, **C71**, 3–8.
- 8 O. V. Dolomanov, L. J. Bourhis, R. J. Gildea, J. A. K. Howard and H. Puschmann, *J. Appl. Cryst.*, 2009, **42**, 339.
- 9 M. J. Frisch, G. W. Trucks, H. B. Schlegel, G. E. Scuseria, M. A. Robb, J. R. Cheeseman, G. Scalmani, V. Barone, B. Mennucci, G. A. Petersson, H. Nakatsuji, M. Caricato, X. Li, H. P. Hratchian, A. F. Izmaylov, J. Bloino, G. Zheng, J. L. Sonnenberg, M. Hada, M. Ehara, K. Toyota, R. Fukuda, J. Hasegawa, M. Ishida, T. Nakajima, Y. Honda, O. Kitao, H. Nakai, T. Vreven, J. A. Montgomery Jr., J. E. Peralta, F. Ogliaro, M. Bearpark, J. J. Heyd, E. Brothers, K. N. Kudin, V. N. Staroverov, R. Kobayashi, J. Normand, K. Raghavachari, A. Rendell, J. C. Burant, S. S. Iyengar, J. Tomasi, M. Cossi, N. Rega, J. M. Millam, M. Klene, J. E. Knox, J. B. Cross, V. Bakken, C. Adamo, J. Jaramillo, R. Gomperts, R. E. Stratmann, O. Yazyev, A. J. Austin, R. Cammi, C. Pomelli, J. W. Ochterski, R. L. Martin, K. Morokuma, V. G. Zakrzewski, G. A. Voth, P. Salvador, J. J. Dannenberg, S. Dapprich, A. D. Daniels, Ö. Farkas, J. B. Foresman, J. V. Ortiz, J. Cioslowski, D. J. Fox, *Gaussian 09, Revision C.01*, Gaussian, Inc., Wallingford, CT, 2010.
- 10 J. P. Perdew, K. Burke and M. Ernzerhof, *Phys. Rev. Lett.*, 1996, **77**, 3865–3868.
- 11 EMSL Basis Set Exchange Library. <https://bse.pnl.gov/bse/portal>
- 12 F. London, *J. Phys. Radium.*, 1937, **8**, 397–409.
- 13 R. Ditchfield, *Mol. Phys.*, 1974, **27**, 789–807.
- 14 K. Wolinski, J. F. Hinton and P. Pulay, *J. Am. Chem. Soc.*, 1990, **112**, 8251–8260.
- 15 (a) A. D. Becke, *Phys. Rev. A.*, 1988, **38**, 3098–3100; (b) C. Lee, W. Yang and R. G. Parr, *Phys. Rev. B.*, 1988, **37**, 785–789; (c) A. D. Becke, *J. Chem. Phys.*, 1993, **98**, 5648–5652.
- 16 T. P. Onak, H. L. Landesman, R. E. Williams and I. Shapiro, *J. Phys. Chem.*, 1959, **63**, 1533–1535.
- 17 (a) E. D. Glendening, A. E. Reed, J. E. Carpenter and F. Weinhold, *NBO Program 3.1*, W. T. Madison, 1988; (b) A. E. Reed, F. Weinhold and L. A. Curtiss, *Chem. Rev.*, 1988, **88**, 899–926; (c) F. Weinhold and R. Landis, *Valency and bonding: A natural bond orbital donor-acceptor perspective*; Cambridge University Press: Cambridge, U.K, 2005.
- 18 K. Wiberg, *Tetrahedron*, 1968, **24**, 1083–1096.
- 19 (a) R. F. W. Bader, *Atoms in Molecules: A Quantum Theory*; Oxford University Press: Oxford, U. K., 1990; (b) R. F. W. Bader, *J. Phys. Chem. A.*, 1998, **102**, 7314–7323; (c) R. F. W. Bader, *Chem. Rev.*, 1991, **91**, 893–928.
- 20 T. Lu, F. Chen, *J. Comput. Chem.*, 2012, **33**, 580–592.
- 21 I. I. Dennington, R. T. Keith, J. Millam, K. Eppinnett, W. L. Hovell and R. Gilliland, *GaussView, Version 3.09*; Semichem Inc.: Shawnee Mission, KS, 2003.
- 22 G. A. Zhurko, <http://www.chemcraftprog.com>.